Reactions of Silicon Atoms with NO. Experimental and Theoretical Characterization of Molecules Containing Si, N, and O

Mingfei Zhou,*,† Ling Jiang,‡ and Qiang Xu*,‡

Department of Chemistry & Laser Chemistry Institute, Shanghai Key Laboratory of Molecular Catalysts and Innovative Materials, Fudan University, Shanghai 200433, People's Republic of China and National Institute of Advanced Industrial Science and Technology (AIST), Ikeda, Osaka 563-8577, Japan

Received: July 4, 2004; In Final Form: August 18, 2004

Reactions of silicon atoms with NO molecules in solid argon have been studied using matrix isolation infrared absorption spectroscopy. The reaction products were identified via isotopic substitutions ($^{15}N^{16}O$, $^{14}N^{18}O$, and mixtures) and comparison with density functional calculations of isotopic frequencies. Three different SiNO isomers: SiNO, NSiO, and Si−η^2-NO were identified. The $Si(NO)_2$ and SiNSiO molecules also were formed on annealing. The SiNO, $Si(NO)_2$, and NSiO molecules decomposed to form the SiO and SiO_2 oxides and the $NNSiO_2$ van der Waals complex upon broad band irradiation.

Introduction

The interaction of metal centers with nitric oxide molecules is of great interest in a wide variety of areas, including surface science, catalytic chemistry, and environmental science. The reaction of silicon with NO is of particular interest in semiconductor construction. Ultrathin silicon oxynitride films are increasingly used as gate dielectric materials.[1,2] One important way to obtain silicon oxynitride films is the rapid thermal oxidation of silicon or silicon oxide in a NO ambient.[2−5] The interactions of NO with silicon atoms, clusters, and surfaces are important in understanding the thermal silicon oxynitridation mechanism. Considerable attention has been focused on the adsorption and reaction of NO on silicon surfaces,[6−9] but much less is known about the reactions of silicon atoms and clusters with NO molecules, which are important in elucidating and modeling the surface reactions. Studies in the gas phase showed that NO reacted readily with all sizes of silicon clusters.[10] Si_4NO^+ and Si_4NO^- cluster isomers, which are possible candidates of $Si_4^{\pm}$ + NO reaction products and/or intermediates, have been theoretically studied.[11] Two distinguishable groups of isomers, NO bond-broken and molecular-adsorbed isomers were found on the potential energy surfaces. The NO bond-broken type is thermodynamically more stable than the molecular-adsorbed type. The silicon nitrosyl SiNO and its isomers NSiO and SiON have been the subject of previous theoretical investigations.[12,13] All of the three isomers were predicted to have a linear conformation with a $^2\Pi$ ground state. Their geometries and vibrational frequencies have been estimated. However, no experimental results have been published on the silicon nitrosyl and its isomers.

In this paper, we report a detailed study of the reactions of silicon atoms with NO in solid argon. The reaction products are identified via isotopic substitutions as well as density functional calculations. We will show that three structural isomers of SiNO, and the SiNSiO and $Si(NO)_2$ molecules, are formed and identified. Photoinduced dissociation of SiNO, $Si(NO)_2$, and NSiO to SiO, SiO_2, and the NN−SiO_2 van der Waals complex are also observed.

Experimental and Computational Methods

The experiment for pulsed laser ablation and matrix isolation infrared spectroscopy is similar to those used previously.[14] Briefly, the Nd:YAG laser fundamental (1064 nm, 10 Hz repetition rate with 10 ns pulse width) was focused on the rotating silicon target. The laser-ablated silicon atoms were codeposited with NO in excess argon onto a CsI window cooled normally to 7 K by means of a closed-cycle helium refrigerator. The matrix gas deposition rate was typically 2−4 mmol per hour. Nitric oxide (Matheson), $^{15}N^{16}O$ (MSD isotopes, 99%), and $^{14}N^{18}O$ (Isotec, 99%) were condensed, and the most volatile fraction was used to prepare the NO/Ar samples. In general, the matrix samples were deposited for 1−2 h. After sample deposition, IR spectra were recorded on a BIO-RAD FTS-6000e spectrometer at 0.5 cm^{-1} resolution using a liquid-nitrogen-cooled HgCdTe (MCT) detector for the spectral range of 5000−400 cm^{-1}. Samples were annealed at different temperatures and subjected to broad band irradiation ($\lambda > 250$ nm) using a high-pressure mercury arc lamp (Ushio, 100 W).

Quantum chemical calculations were performed to predict the structures and vibrational frequencies of the observed reaction products using the Gaussian 98 program.[15] The Becke's three parameter hybrid functional with the Lee−Yang−Parr correlation corrections (B3LYP) was used.[16,17] The 6-311+G-(d) basis set was used for the Si, N, and O atoms.[18] Geometries were fully optimized and vibrational frequencies calculated with analytical second derivatives.

Results and Discussions

Infrared Spectra. Series of experiments have been done using different NO concentrations (ranging from 0.025 to 0.2% in argon) and different laser energies (ranging from 5 to 20 mJ/pulse). The infrared spectra in the 1650−950 cm^{-1} region, which contains at least one absorption of each product from codeposition of laser-ablated silicon atoms and 0.05% NO in argon, are shown in Figure 1, and the product absorptions are listed in

* E-mail: mfzhou@fudan.edu.cn (Zhou), q.xu@aist.go.jp (Xu).
† Fudan University.
‡ National Institute of Advanced Industrial Science and Technology.

10.1021/jp047057i CCC: $27.50
Published on Web 10/09/2004

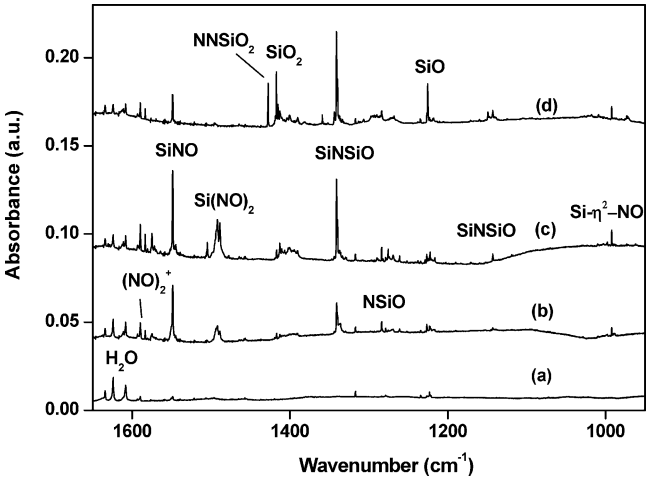

Figure 1. Infrared spectra in the 1650−950 cm^{-1} region from codeposition of laser-ablated silicon atoms and 0.05% NO in argon. (a) After 1 h of sample deposition at 7 K, (b) after annealing to 25 K, (c) after annealing to 30 K, and (d) after 20 min of broad-band irradiation.

TABLE 1: Infrared Absorptions (cm^{-1}) from the Reactions of Silicon Atoms with NO in Solid Argon

$^{14}N^{16}O$	$^{15}N^{16}O$	$^{14}N^{18}O$	assignment
1825.6	1793.3	1778.7	$Si_x(NO)_y$
1662.6	1631.8	1627.9	$Si_x(NO)_y$
1548.7	1522.8	1518.3	SiNO
1504.6	1479.5	1463.6	$Si_x(NO)_y$
1492.0	1464.9	1451.6	$Si(NO)_2$
1427.7	1427.7	1390.6	$NNSiO_2$
1417.2	1417.2	1380.5	SiO_2
1340.9	1307.8	1340.3	SiNSiO
1283.8	1280.1	1254.7	NSiO
1225.3	1225.3	1181.4	SiO
1142.8	1141.4	1107.2	SiNSiO
992.1	979.7	969.1	Si−η^2-NO
755.4	751.0	740.1	SiNO
710.6	699.5	701.3	Si−η^2-NO
580.3	578.4	577.4	SiNSiO

Table 1. Bands due to NO, $(NO)_2$, and other common nitric oxide species including N_2O, $(NO)_2^+$, and $(NO)_2^-$ were also observed[19,20] and are not listed in Table 1. The stepwise annealing and photolysis behavior of the new product absorptions are also shown in the figure and will be discussed below.

Different isotopic nitric oxides: $^{15}N^{16}O$, $^{14}N^{18}O$, and $^{14}N^{16}O + {}^{15}N^{16}O$, and $^{14}N^{16}O + {}^{14}N^{18}O$ mixtures were employed for product identification through isotopic shifts and splittings. The isotopic counterparts are also listed in Table 1. The mixed $^{14}N^{16}O + {}^{15}N^{16}O$ spectra in the 1600−1250 cm^{-1} frequency region are shown in Figure 2,, and the mixed $^{14}N^{16}O + {}^{14}N^{18}O$ spectra in the 1600−1320 cm^{-1} frequency region are illustrated in Figure 3. Figures 4−6 show the spectra in the 1160−960, 770−730, and 590−570 cm^{-1} regions for different isotopic NO samples after 30 K annealing.

Calculation Results. Quantum chemical calculations were performed on the potential product molecules. Four different geometric SiNO isomers were calculated, namely, nitrosyl SiNO, isonitrosyl SiON, side-bonded Si−η^2-NO and inserted NSiO molecules. The optimized structures and relative stability are shown in Figure 7. The vibrational frequencies and intensities are listed in Table 2. All of the four SiNO isomers were predicted to be stable relative to the ground state Si atom and NO molecule, and all have a doublet ground state. In agreement with the previous theoretical calculations,[12,13] the SiNO, NSiO, and SiON molecules were predicted to have a $^2\Pi$ ground state

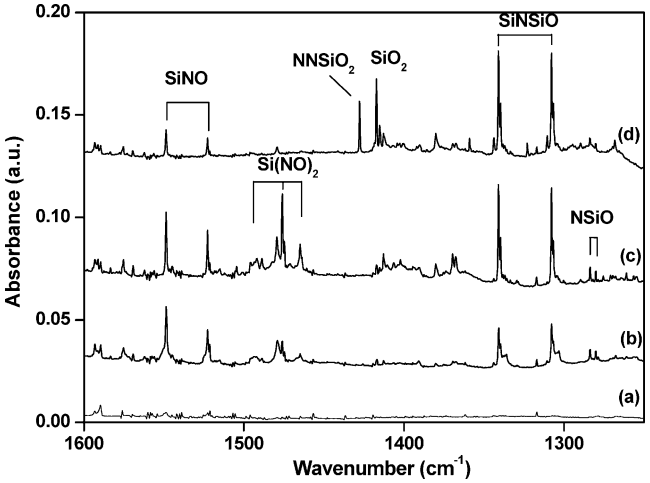

Figure 2. Infrared spectra in the 1600−1250 cm^{-1} region from codeposition of laser-ablated silicon atoms and 0.03% $^{14}N^{16}O$ + 0.03% $^{15}N^{16}O$ in argon. (a) After 1 h of sample deposition at 7 K, (b) after annealing to 25 K, (c) after annealing to 30 K, and (d) after 20 min of broad-band irradiation.

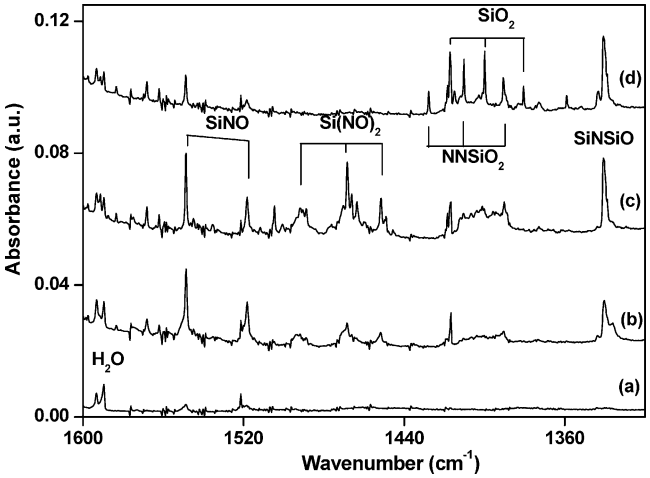

Figure 3. Infrared spectra in the 1600−1320 cm^{-1} region from codeposition of laser-ablated silicon atoms and 0.03% $^{14}N^{16}O$ + 0.03% $^{14}N^{18}O$ in argon. (a) After 1 h of sample deposition at 7 K, (b) after annealing to 25 K, (c) after annealing to 30 K, and (d) after 20 min of broad band irradiation.

with a linear structure. The side-bonded Si−η^2-NO molecule was calculated to have a $^2A''$ ground state. The SiNO nitrosyl is the global minimum, and the Si−η^2-NO, NSiO, and SiON isomers are 7.1, 9.2, and 41.8 kcal/mol higher in energy.

Similar calculations were also performed for Si_2NO, $Si(NO)_2$, and $NNSiO_2$ molecules. Two distinguishable groups of isomers, NO bond-broken and molecular-adsorbed isomers with Si_2NO formulas were computed. For NO molecular-adsorbed isomers, the most stable structure was predicted to have a semibridge-bonded structure with two inequivalent Si−N bonds (1.733 and 1.881 Å). A number of NO bond-broken isomers, including SiNSiO, NSiSiO, SiOSiN, and cyclic-$Si_2(\mu\text{-N})(\mu\text{-O})$ were also calculated. The most stable structure is a bent *trans*-SiNSiO structure, which was predicted to be more stable than the semibridge-bonded Si_2NO by about 12.2 kcal/mol. We have optimized singlet, triplet, and quintet spin states for $Si(NO)_2$ with a bent C_{2v} symmetry. The most stable structure was found to be a $^3B_2$ state. The optimized structures for Si_2NO, SiNSiO, $Si(NO)_2$, and $NNSiO_2$ are shown in Figure 8, and the vibrational frequencies and intensities are listed in Table 2. Table 3 provides

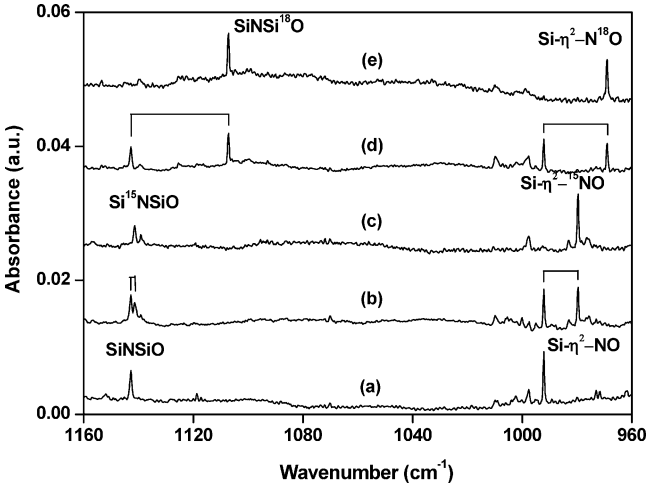

Figure 4. Infrared spectra in the 1160−960 cm^{-1} region from codeposition of laser-ablated silicon atoms and NO in excess argon. Spectra were taken after 30 K annealing. (a) 0.05% $^{14}N^{16}O$, (b) 0.03% $^{14}N^{16}O$ + 0.03% $^{15}N^{16}O$, (c) 0.05% $^{15}N^{16}O$, (d) 0.03% $^{14}N^{16}O$ + 0.03% $^{14}N^{18}O$, and (e) 0.05% $^{14}N^{18}O$.

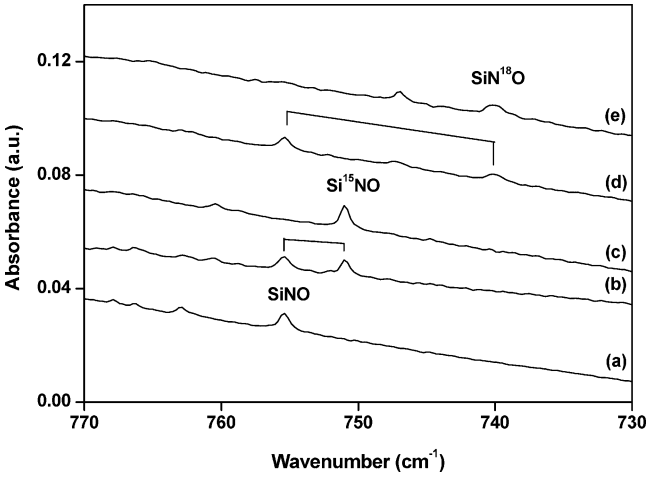

Figure 5. Infrared spectra in the 770−730 cm^{-1} region from codeposition of laser-ablated silicon atoms and NO in excess argon. Spectra were taken after 30 K annealing. (a) 0.05% $^{14}N^{16}O$, (b) 0.03% $^{14}N^{16}O$ + 0.03% $^{15}N^{16}O$, (c) 0.05% $^{15}N^{16}O$, (d) 0.03% $^{14}N^{16}O$ +0.03% $^{14}N^{18}O$, and (e) 0.05% $^{14}N^{18}O$.

a comparison of observed and calculated isotopic frequency ratios for the observed product absorptions.

SiNO. As shown in Figure 1, the 1548.7 cm^{-1} absorption appeared on 25 K annealing, increased on 30 K annealing, but greatly decreased on broad band irradiation. This band shifted to 1522.8 cm^{-1} with $^{15}N^{16}O$ and to 1518.3 cm^{-1} with $^{14}N^{18}O$. The isotopic $^{14}N/^{15}N$ ratio of 1.0170 and $^{16}O/^{18}O$ ratio of 1.0200 suggest that this band is due to the N−O stretching mode of a nitrosyl species. In the mixed $^{14}N^{16}O$ + $^{15}N^{16}O$ and $^{14}N^{16}O$ + $^{14}N^{18}O$ experiments (Figures 2 and 3), only the pure isotopic counterparts were observed, which indicate that only one NO subunit is involved in this mode, and thus the 1548.7 cm^{-1} band is assigned to the SiNO molecule. A weak band at 755.4 cm^{-1} tracked with the 1548.7 cm^{-1} band. This band shifted to 751.0 and 740.1 cm^{-1}, respectively, with the $^{15}N^{16}O$ and $^{14}N^{18}O$ samples, giving the isotopic $^{14}N/^{15}N$ ratio of 1.0059 and $^{16}O/^{18}O$ ratio of 1.0207. This band is assigned to the Si−N stretching mode of SiNO.

The SiNO assignment is supported by DFT calculations. The N−O and Si−N stretching modes of ground state SiNO were computed at 1589.1 and 777.0 cm^{-1}, which are 2.5 and 2.8% higher than the experimental values. As listed in Table 3, the calculated isotopic frequency ratios for both modes are very close to the observed values. The bending mode of SiNO was predicted at 320.7 cm^{-1}, which is out of the detection range of our spectrometer.

The $^2\Pi$ ground-state SiNO molecule was predicted to have Si−N and N−O bond lengths of 1.629 and 1.210 Å. The Si−N bond length is shorter than that of Si−N single bonded aminosilylene $HSiNH_2$ (1.725 Å) and is close to that of Si−N double-bonded H_2SiNH (1.603 Å) calculated at the same level,[21] which suggests that the Si−N bond in SiNO can be regarded as a double bond. The N−O bond length of 1.210 Å is of the order of a N−O double bond. The bond lengths of NO and NO^- were predicted to be 1.148 and 1.264 Å, respectively.

Si−η^2-NO. The band at 992.1 cm^{-1} appeared on 25 K annealing, markedly increased on 30 K annealing, and slightly decreased on broad band irradiation. This band shifted to 979.7

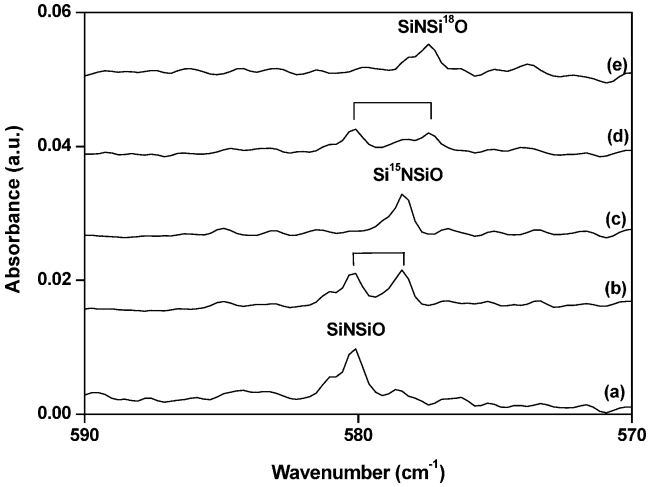

Figure 6. Infrared spectra in the 590−570 cm^{-1} region from codeposition of laser-ablated silicon atoms and NO in excess argon. Spectra were taken after 30 K annealing. (a) 0.05% $^{14}N^{16}O$, (b) 0.03% $^{14}N^{16}O$ + 0.03% $^{15}N^{16}O$, (c) 0.05% $^{15}N^{16}O$, (d) 0.03% $^{14}N^{16}O$ +0.03% $^{14}N^{18}O$, and (e) 0.05% $^{14}N^{18}O$.

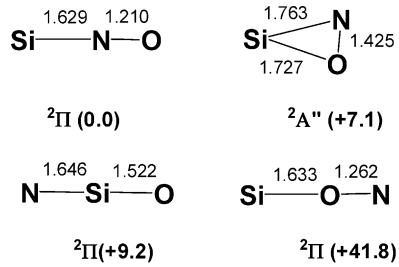

Figure 7. Optimized structures (bond lengths in Å) and relative stability (values in parentheses, in kcal/mol) of the SiNO isomers.

TABLE 2: Calculated Vibrational Frequencies (cm^{-1}) and Intensities (km/mol) for the Product Species

molecule	frequency (intensity, mode)
SiNO ($^2\Pi$)	1589.1 (316, σ), 777.0 (38, σ), 320.7 (21, π)
NSiO ($^2\Pi$)	1307.3 (42, σ), 877.6 (2, σ), 206.2 (129, π)
Si−η^2-NO ($^2A''$)	1030.4 (55, a′), 722.9 (27, a′), 563.4 (5, a′)
SiON ($^2\Pi$)	1151.7 (241, σ), 730.2 (25, σ), 302.5 (9, π)
SiNSiO ($^2A'$)	1343.4 (380, a′), 1137.6 (27, a′), 561.4 (38, a′), 333.1(34, a′), 168.7 (7, a″), 126.6 (3, a′)
$Si(NO)_2$ ($^3B_2$)	1745.3 (162, a_1), 1618.5 (1272, b_2), 617.4 (25, a_1), 478.2 (49, b_2), 475.7 (0, a_2), 369.3 (1, a_1), 323.4 (4, b_2), 162.3 (1, a_1), 156.7 (0, b_1)
$NNSiO_2$ ($^1A_1$)	2451.4 (3, a_1), 1443.9 (116, b_2), 991.4 (1, a_1), 287.1 (82, b_1), 284.2 (142, a_1), 133.0 (0, b_2), 78.0 (1, b_1), 54.7 (6, a_1), 29.7 (0, b_2)

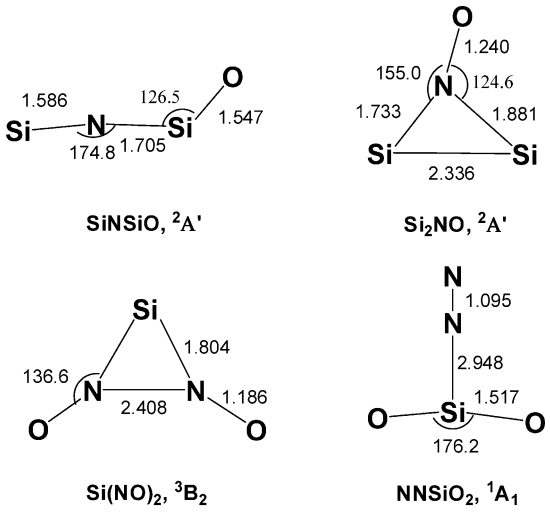

Figure 8. Optimized structures (bond lengths in Å, bond angles in degrees) of the Si_2NO, SiNSiO, $Si(NO)_2$, and $NNSiO_2$ molecules.

TABLE 3: Comparison of the Observed and Calculated Isotopic Frequency Ratios of the Reaction Products

		$^{14}N/^{15}N$		$^{16}O/^{18}O$	
molecule	mode	obsd	calcd	obsd	calcd
SiNO	N−O str.	1.0170	1.0217	1.0200	1.0199
	Si−N str.	1.0059	1.0044	1.0207	1.0226
NSiO	Si−O str.	1.0029	1.0029	1.0232	1.0234
Si(η^2-NO)	N−O str.	1.0127	1.0137	1.0237	1.0257
	Si−N str.	1.0159	1.0167	1.0133	1.0110
SiNSiO	Si−N str.	1.0253	1.0261	1.0004	1.0003
	Si−O str.	1.0012	1.0008	1.0322	1.0354
	bending	1.0033	1.0020	1.0050	1.0045
$Si(NO)_2$	N−O asym-str.	1.0185	1.0173	1.0278	1.0285
$NNSiO_2$	SiO_2 asym-str.	1.0000	1.0000	1.0267	1.0270

cm^{-1} with $^{15}N^{16}O$ and to 969.1 cm^{-1} with $^{14}N^{18}O$. The isotopic frequency ratios ($^{14}N/^{15}N$: 1.0127 and $^{16}O/^{18}O$: 1.0237) are slightly lower than those of diatomic NO, but still indicate a N−O stretching mode. Doublets were observed in the mixed $^{14}N^{16}O + {}^{15}N^{16}O$ and $^{14}N^{16}O + {}^{14}N^{18}O$ experiments (Figure 4), and another SiNO isomer should be considered. The band position is too low for a terminal-bonded nitrosyl but is appropriate for a side-bonded species.[22] Therefore, we assign the 992.1 cm^{-1} band to the N−O stretching mode of the side-bonded Si−η^2-NO molecule. A very weak band at 710.6 cm^{-1} showed the same annealing and photolysis behavior and is assigned to the Si−N stretching mode of Si-η^2-NO. The $^{15}N^{16}O$ and $^{14}N^{18}O$ counterparts of this mode were observed at 699.5 and 701.3 cm^{-1}.

The N−O and Si−N stretching modes of the $^2A''$ ground-state Si−η^2-NO molecule were predicted at 1030.4 and 722.9 cm^{-1}, which are 3.7 and 1.7% higher than the experimental values. As listed in Table 3, the calculated isotopic frequency ratios for both modes are in quite good agreement with the observed values. The Si−O stretching mode was predicted at 563.4 cm^{-1} with much lower IR intensity (5 km/mol versus 55 and 27 km/mol for the N−O and Si−N stretching modes). This mode was too weak to be observed in the experiments.

The side-bonded Si−η^2-NO molecule is the second stable isomer; it lies only about 7.1 kcal/mol higher in energy than the linear SiNO molecule. The N−O bond length was predicted to be 1.425 Å, which is only slightly shorter than that of a typical N−O single bond (1.44 Å),[23] suggesting that the N−O bond in Si−η^2-NO is a single bond. The Si−N and Si−O bond lengths were predicted to be 1.763 and 1.727 Å, both exhibiting single bond character.

NSiO. The band at 1283.8 cm^{-1} appeared and increased on annealing, but disappeared on broad band irradiation. This band showed very small nitrogen isotopic shift (3.7 cm^{-1}) with the $^{15}N^{16}O$ sample, but shifted to 1254.7 cm^{-1} with the $^{14}N^{18}O$ sample. The isotopic $^{16}O/^{18}O$ ratio of 1.0232 and $^{14}N/^{15}N$ ratio of 1.0029 imply that the 1283.8 cm^{-1} band is mainly due to a Si−O stretching mode, but is coupled by N atom(s). In the mixed $^{14}N^{16}O + {}^{15}N^{16}O$ and $^{14}N^{16}O + {}^{14}N^{18}O$ experiments, only the pure isotopic counterparts were presented, indicating that only one N atom and one O atom are involved in this mode. Accordingly, a NSiO molecule is suggested.

DFT calculations confirmed this assignment and predicted a $^2\Pi$ ground state for the linear NSiO molecule, which lies 9.2 kcal/mol higher in energy than the linear SiNO isomer. The NSiO molecule has three vibrational fundamentals: Si−O and Si−N stretching and bending vibrations, which were calculated at 1307.3, 877.6, and 206.2 cm^{-1} with 42, 2, and 129 km/mol IR intensities. The calculated Si−O stretching frequency is only 1.8% higher than the observed value. The Si−N stretching mode was predicted to have very low IR intensity and was not observed in the experiments. The bending mode has large IR intensity, but the frequency is out of the detection range of our spectrometer. The calculated isotopic ratios for the observed mode are in excellent agreement with the experimental ratios (Table 3). It is interesting to note that the isotopic $^{16}O/^{18}O$ ratio of the Si−O stretching mode is much smaller than the diatomic SiO ratio (1.0372) and is close to the ratio of the antisymmetric Si−O stretching mode of SiO_2 (1.0266). The Si−O and Si−N stretching modes in NSiO are strongly coupled, and, therefore, are better described as the antisymmetric and symmetric stretching vibrations.

The Si−N and Si−O bond lengths of the ground state NSiO molecule were predicted to be 1.646 and 1.522 Å. Both bonds can be regarded as double bonds. The spin density is mainly located on the N atom, and, therefore, doublet NSiO is a linear univalent radical. The Lewis structure can be drawn as •N═Si═O, which satisfies the valence of silicon.

SiNSiO. Absorptions at 1340.9, 1142.8, and 580.3 cm^{-1} appeared together on annealing. These absorptions are favored in low NO concentration and high laser power experiments, suggesting the involvement of more than one silicon atom. The 1340.9 cm^{-1} band showed very small shift with $^{14}N^{18}O$ (0.6 cm^{-1}) but shifted to 1307.8 cm^{-1} with $^{15}N^{16}O$. The $^{14}N/^{15}N$ isotopic frequency ratio of 1.0253 implies that this band is mainly due to a Si−N stretching vibration (The harmonic ratio of diatomic SiN was calculated to be 1.0230). In contrast, the 1142.8 cm^{-1} band shifted to 1141.4 cm^{-1} with $^{15}N^{16}O$ and to 1107.2 cm^{-1} with $^{14}N^{18}O$, which define a small $^{14}N/^{15}N$ ratio (1.0012) and a large $^{16}O/^{18}O$ ratio (1.0322). These ratios show that the 1142.8 cm^{-1} band is mostly Si−O stretching in vibrational character. The 580.3 cm^{-1} band shifted to 578.4 cm^{-1} with $^{15}N^{16}O$ and to 577.4 cm^{-1} with $^{14}N^{18}O$ and is due to a bending vibration. The mixed $^{14}N^{16}O + {}^{15}N^{16}O$ and $^{14}N^{16}O + {}^{14}N^{18}O$ isotopic spectra (Figures 2, 4, and 6) each reveal only two isotopic bands and clearly indicate that only one N and one O atom are involved in these modes. Analogous to the BNBO molecule,[24] these three absorptions are assigned to the Si−N and Si−O stretching vibrations, and to the bending vibrations of the SiNSiO molecule.

The calculated frequencies at the optimized geometry of SiNSiO provide excellent support for the assignment. The three experimentally observed modes were predicted at 1343.4, 1137.6 and 561.4 cm^{-1}, which are 2.5, −5.2, and −18.9 cm^{-1} from

the observed values. The isotopic frequency shifts were also predicted correctly (Table 3).

The observed Si−N stretching frequency (1340.9 cm^{-1}) is significantly higher than that of SiNO and is even higher than those of SiN (1144 cm^{-1}),[25] HSiN (1163 cm^{-1}),[26] and SiNH (1202 cm^{-1}).[27] The Si−O stretching frequency (1142.8 cm^{-1}) is ca. 82.5 cm^{-1} lower than that of SiO in solid argon. Unlike the linear BNBO molecule, the ground state of SiNSiO was predicted to have a bent structure with the SiNSi and NSiO bond angles of 174.8 and 126.5°. The terminal Si−N bond length of 1.586 Å is shorter than those of SiNO and NSiO and is close to those of SiNH (1.559 Å) and HSiN (1.565 Å) with a typical Si−N triple bond.[21] The population analysis shows that the spin is predominately on the O-linked Si atom, and doublet SiNSiO can also be regarded as a univalent radical. The valence bond structure can be drawn as Si≡N−Si═O.

$Si(NO)_2$. An absorption at 1492.0 cm^{-1} appeared on 25 K annealing, greatly increased on subsequent 30 K annealing, and disappeared on broad band irradiation. The band is favored in high NO concentration experiments. It shifted to 1464.9 cm^{-1} with $^{15}N^{16}O$ and to 1451.6 cm^{-1} with $^{14}N^{18}O$. The isotopic frequency ratios ($^{14}N/^{15}N$: 1.0185, $^{16}O/^{18}O$: 1.0278) indicate that this band is due to a N−O stretching mode. This band formed a triplet at 1492.0, 1476.1, and 1464.9 cm^{-1} with the mixed $^{14}N^{16}O + {}^{15}N^{16}O$ sample (Figure 2). Similar triplets at 1492.0, 1468.4, and 1451.6 cm^{-1} were produced with the mixed $^{14}N^{16}O + {}^{14}N^{18}O$ sample (Figure 3). The mixed isotopic spectra clearly indicate that two equivalent NO subunits are involved in this molecule. Therefore, we assign the 1492.0 cm^{-1} band to the $Si(NO)_2$ molecule.

The $Si(NO)_2$ molecule was predicted to have a $^3B_2$ ground state with a bent structure. The antisymmetric NO stretching mode was computed at 1618.5 cm^{-1}, with the isotopic frequency ratios in good agreement with the observed values (Table 3). The symmetric NO stretching mode was predicted at 1745.3 cm^{-1}, with much lower intensity (about 13% of the intensity of the antisymmetric stretching mode). The $^3B_2$ ground-state $Si(NO)_2$ molecule can be regarded as bonding between a Si atom and a $(NO)_2$ dimer. The molecule was predicted to have a very acute NSiN bond angle (83.7°). The N−N bond distance of 2.408 Å is slightly longer than that in cis-$(NO)_2$.[28]

$NNSiO_2$. Absorptions at 1417.2 and 1427.7 cm^{-1} were observed on broad band irradiation during which the $Si(NO)_2$ absorptions disappeared. Both bands exhibited no nitrogen isotopic shifts with $^{15}N^{16}O$, but shifted to 1390.6 and 1380.5 cm^{-1} with a $^{14}N^{18}O$ sample. When a 1:1 mixture of $^{14}N^{16}O + {}^{14}N^{18}O$ was used, both bands split into triplets with intensity ratios of approximately 1:2:1, indicating that two equivalent O atoms are involved. The isotopic $^{16}O/^{18}O$ ratios (1.0267 and 1.0266) indicate that both bands are due to antisymmetric SiO_2 stretching vibrations. According to the previous studies, the 1417.2 cm^{-1} band is due to the antisymmetric stretching mode of linear SiO_2 in solid argon.[29,30] The 1427.7 cm^{-1} band is about 10.5 cm^{-1} blue shifted from that of SiO_2 and is assigned to the $NNSiO_2$ complex. Present B3LYP calculations on $NNSiO_2$ predicted a van der Waals complex with a T-shaped C_{2v} structure. The Si−N distance was predicted to be 2.948 Å. The antisymmetric SiO_2 stretching frequency of $NNSiO_2$ was calculated to be slightly shifted from that of SiO_2.

Other Absorptions. Absorptions at 1826.5, 1662.6, and 1504.6 cm^{-1} appeared on annealing, disappeared upon broad band irradiation, and increased on later annealing. These absorptions are favored in high NO concentration experiments, suggesting the involvement of more than one NO. All of these absorptions exhibited isotopic frequency shifts for the NO stretching vibrations. These absorptions cannot be identified and are simply labeled "$Si_x(NO)_y$" in Table 1.

Reaction Mechanisms. Three structural isomers of SiNO were observed in the experiments. The SiNO and Si−η^2-NO absorptions increased on annealing, suggesting that the addition reactions 1 and 2 proceed with little or no activation energy. Although the side-bonded structure is 7.1 kcal/mol less stable than the linear SiNO isomer, both structures are stable with respect to the ground state reactants: Si + NO. The energy barrier from the side-bonded structure to the linear structure was predicted to be 25.3 kcal/mol. Both the end-on and side-bonded addition products were formed in a number of transition metal atom and NO reactions in solid matrix.[22]

$$Si + NO \rightarrow SiNO \quad (1)$$

$$Si + NO \rightarrow Si\text{-}\eta^2\text{-}NO \quad (2)$$

The NSiO insertion molecule was also observed to grow on annealing. Since both the SiNO and Si−η^2-NO isomers were observed to increase on annealing, the silicon atom insertion to form NSiO requires activation energy. The growth of NSiO on annealing is probably due to diffusion and reaction of N or O atoms. Some of the NO molecules dissociated during the ablation/condensation process. The N_2O absorptions increased on annealing presumably because of N atom reaction with NO. Although no evidence was found for the formation of SiN, weak SiO absorption was clearly observed after sample deposition and decreased on annealing. We note that the NSiO absorption increased more on annealing after broad band irradiation, during which the SiNO absorptions were almost destroyed to produce strong SiO absorption. Although SiNO is more stable than NSiO, the N atom prefers to interact with SiO at the Si side to form NSiO. The SiON isomer was not observed in the present experiments. This isomer was predicted to lie 41.8 kcal/mol higher in energy than the most stable SiNO isomer. The ground state SiON molecule was predicted to have a strong O−N stretching vibration at 1151.7 cm^{-1}.

The absorptions due to SiNSiO also increased on annealing. This molecule may be formed either via Si and NSiO addition reaction 3 or via silicon dimer and NO reaction 4. The SiNSiO molecule was predicted to be 12.2 kcal/mol more stable than the Si_2NO isomer. The Si_2NO isomer was not observed in the experiments, which suggests that Si_2 may directly react with NO to form SiNSiO.

$$Si + NSiO \rightarrow SiNSiO \quad (3)$$

$$Si_2 + NO \rightarrow SiNSiO \quad (4)$$

The absorption due to the $Si(NO)_2$ molecule increased on annealing. This molecule is most probably formed via the reaction of a Si atom and $(NO)_2$, reaction 5, which was predicted to be exothermic. The $Si(NO)_2$ absorption decreased on broad band irradiation, during which the SiO_2 and $NNSiO_2$ absorptions appeared. This observation suggests that $Si(NO)_2$ underwent photoinduced isomerization or dissociation to $NNSiO_2$ or SiO_2, as shown in reaction 6. The $NNSiO_2$ van der Waals complex was predicted to be 124.5 kcal/mol lower in energy than the $Si(NO)_2$ isomer.

$$Si + (NO)_2 \rightarrow Si(NO)_2 \quad (5)$$

$$Si(NO)_2 + h\nu \rightarrow NNSiO_2 \text{ or } SiO_2 + N_2 \quad (6)$$

Besides the $Si(NO)_2$ absorptions, the SiNO and NSiO absorptions also disappeared or decreased on broad band irradiation, during which the SiO absorption greatly increased. It appears that SiNO and NSiO underwent UV−visible light induced dissociation to form SiO. However, the SiNSiO absorptions kept almost unchanged upon irradiation, which suggests that the SiNSiO molecule is stable under UV−visible irradiation.

Conclusions

Reactions of silicon atoms with NO molecules in solid argon have been studied using matrix isolation infrared absorption spectroscopy. Absorptions due to SiNO (1548.7 and 755.4 cm^{-1}), Si−η^2-NO (992.1 and 710.6 cm^{-1}), and NSiO (1283.8 cm^{-1}) were observed and identified via isotopic substitutions ($^{15}N^{16}O$, $^{14}N^{18}O$, and mixtures) and density functional calculations. The SiNO and Si−η^2-NO molecules were formed by addition reactions upon diffusion of ground state reagents in solid argon. The NSiO insertion product was probably produced via diffusion and reaction of N or O atoms. The $Si(NO)_2$ and SiNSiO molecules were also formed upon annealing. On broad band irradiation, the SiNO, $Si(NO)_2$, and NSiO molecules decomposed to form the SiO and SiO_2 oxides, as well as the $NNSiO_2$ van der Waals complex.

Acknowledgment. This work is supported by NSFC (Grant 20125311), the NKBRSF of China, the JSPS, and the NEDO of Japan.

References and Notes

(1) Wilk, G. D.; Wallace, R. M.; Anthony, J. M. *J. Appl. Phys*. **2001**, *89*, 5243.

(2) Green, M. L.; Gusev, E. P.; Degraeve, R.; Garfunkel, E. L. *J. Appl. Phys*. **2001**, *90*, 2057.

(3) Yao, Z. Q.; Harrison, H. B.; Dimitrijev, S.; Sweatman, D.; Yeow, Y. T. *Appl. Phys. Lett.* **1994**, *64*, 3584.

(4) Scheer, K. C.; Rao, R. A.; Muralidhar, R.; Bagchi, S.; Conner, J.; Lozano, L.; Perez, C.; Sadd, M.; White, B. E. *J. Appl. Phys.* **2003**, *93*, 3615.

(5) De Almeida, R. M. C.; Baumvol, I. J. R.; Ganem, J. J.; Trimaille, I.; Rigo, S. *J. Appl. Phys*. **2004**, *95*, 1770.

(6) Rangelov, G.; Stober, J.; Eisenhut, B.; Fauster, T. *Phys. Rev. B* **1991**, *44*, 1954.

(7) Korkin, A. A.; Demkov, A. A.; Tanpipat, N.; Andzelm, J. *J. Chem. Phys*. **2000**, *113*, 8237.

(8) Hellner, L.; Comtet, G.; Ramage, M. J.; Bobrov, K.; Carbone, M.; Dujardin, G. *J. Chem. Phys.* **2003**, *119*, 515.

(9) Kim, Y. K.; Ahn, J. R.; Choi, W. H.; Lee, H. S.; Yeom, H. W. *Phys. Rev. B* **2003**, *68*, 075323. Chung, Y. D.; Kim, J. W.; Whang, C. N.; Yeom, H. W. *Phys. Rev. B* **2002**, *65*, 155310.

(10) Elkind, J. L.; Alfold, J. M.; Weiss, F. D.; Laaksonen, R. T.; Smalley, R. E. *J. Chem. Phys*. **1987**, *87*, 2397.

(11) Wang, W. N.; Tang, H. R.; Fan, K. N.; Iwata, S. *Chem. Phys. Lett*. **1999**, *310*, 313. Wang, W. N.; Fan, K. N.; Iwata, S. *Chem. Phys. Lett.* **1997**, *273*, 337.

(12) Fan, K.; Iwata, S. *Chem. Phys. Lett*. **1992**, *189*, 401.

(13) Puzzarini, C.; Tarroni, R.; Palmieri, P.; Cartes, S. *J. Chem. Soc., Faraday Trans.* **1996**, *92*, 4361.

(14) Chen, M. H.; Wang, X. F.; Zhang, L. N.; Yu, M.; Qin, Q. Z. *Chem. Phys*. **1999**, *242*, 81. Zhou, M. F.; Tsumori, N.; Andrews, L.; Xu, Q. *J. Phys. Chem. A* **2003**, *107*, 2458.

(15) Frisch, M. J.; Trucks, G. W.; Schlegel, H. B.; Scuseria, G. E.; Robb, M. A.; Cheeseman, J. R.; Zakrzewski, V. G.; Montgomery, J. A., Jr.; Stratmann, R. E.; Burant, J. C.; Dapprich, S.; Millam, J. M.; Daniels, A. D.; Kudin, K. N.; Strain, M. C.; Farkas, O.; Tomasi, J.; Barone, V.; Cossi, M.; Cammi, R.; Mennucci, B.; Pomelli, C.; Adamo, C.; Clifford, S.; Ochterski, J.; Petersson, G. A.; Ayala, P. Y.; Cui, Q.; Morokuma, K.; Malick, D. K.; Rabuck, A. D.; Raghavachari, K.; Foresman, J. B.; Cioslowski, J.; Ortiz, J. V.; Baboul, A. G.; Stefanov, B. B.; Liu, G.; Liashenko, A.; Piskorz, P.; Komaromi, I.; Gomperts, R.; Martin, R. L.; Fox, D. J.; Keith, T.; Al-Laham, M. A.; Peng, C. Y.; Nanayakkara, A.; Gonzalez, C.; Challacombe, M.; Gill, P. M. W.; Johnson, B.; Chen, W.; Wong, M. W.; Andres, J. L.; Gonzalez, C.; Head-Gordon, M.; Replogle, E. S.; Pople, J. A. *Gaussian 98*, revision A.7; Gaussian, Inc.: Pittsburgh, PA, 1998.

(16) Becke, A. D. *J. Chem. Phys.* **1993**, *98*, 5648.

(17) Lee, C.; Yang, E.; Parr, R. G. *Phys. Rev. B* **1988**, *37*, 785.

(18) McLean, A. D.; Chandler, G. S. *J. Chem. Phys.* **1980**, *72*, 5639. Krishnan, R.; Binkley, J. S.; Seeger, R.; Pople, J. A. *J. Chem. Phys.* **1980**, *72*, 650.

(19) Andrews, L.; Zhou, M. F.; Willson, S. P.; Kushto, G. P.; Snis, A.; Panas, I. *J. Chem. Phys*. **1998**, *109*, 177.

(20) Hacaloglu, J.; Suzer, S.; Andrews, L. *J. Phys. Chem.* **1990**, *94*, 1759. Jacox, M. E.; Thompson, W. E. *J. Chem. Phys*. **1990**, *93*, 7609. Strobel, A.; Knoblauch, N.; Agreiter, J.; Smith, A. M.; Neiderschatteburg, G.; Bondybey, V. E. *J. Phys. Chem.* **1995**, *99*, 872.

(21) Chen, M. H.; Zeng, A. H.; Lu, H.; Zhou, M. F. *J. Phys. Chem. A* **2002**, *106*, 3077, and references therein.

(22) Zhou, M. F.; Andrews, L. *J. Phys. Chem. A* **1998**, *102*, 7452. Zhou, M. F.; Andrews, L. *J. Phys. Chem. A* **1999**, *103*, 478.

(23) Pauling, L. *The Nature of the Chemical Bond*, third ed.; Cornell University Press: New York, 1960, p 344.

(24) Zhou, M. F.; Tsumori, N.; Xu, Q.; Kushto, G. P.; Andrews, L. *J. Am. Chem. Soc.* **2003**, *125*, 11371.

(25) Mullikan, R. S. *Phys. Rev.* **1925**, *26*, 319.

(26) Maier, G.; Glatthaar, J. *Angew. Chem., Int. Ed. Engl*. **1994**, *33*, 473.

(27) Ogilvie, J. F.; Cradock, S. *J. Chem. Soc. Chem. Commun*. **1966**, 364.

(28) McKellar, A. R.; Watson, J. K. G.; Howard, B. J. *Mol. Phys*. **1995**, *86*, 273. Snis, A.; Panas, I. *Chem. Phys.* **1997**, *221*, 1.

(29) Anderson, J. S.; Ogden, J. S. *J. Chem. Phys*. **1969**, *51*, 4189. Schnockel, H. *Angew. Chem.* **1978**, *90*, 638.

(30) Andrews, L.; McCluskey, M. *J. Mol. Spectrosc*. **1992**, *154*, 223. Miao, L.; Shao, L. M.; Wang, W. N.; Fan, K. N.; Zhou, M. F. *J. Chem. Phys.* **2002**, *116*, 5643.